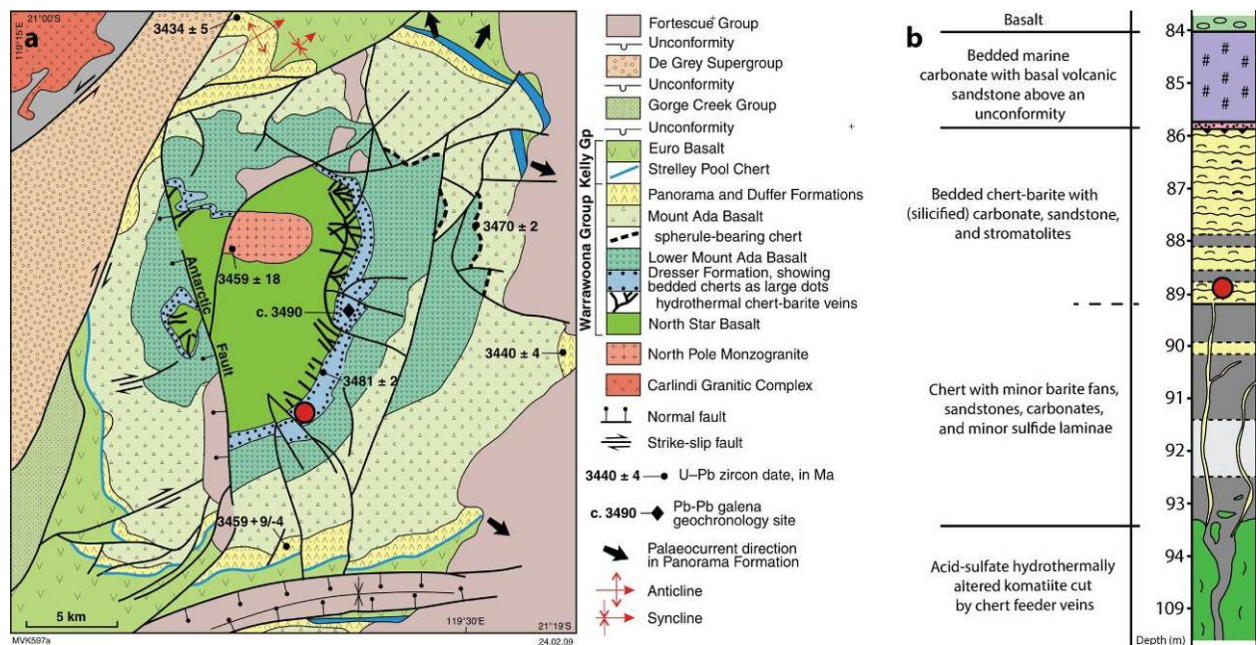Figure DR1. Geology of the Dresser Formation at North Pole Dome, Pilbara Craton, Western Australia, and stratigraphic position of the stromatolites examined in this study. a) Geology at North Pole Dome (redrawn after Van Kranendonk et al., 2008). The red circle indicates the PDP2 drilling site. b) Log of the PDP2b drillcore (redrawn after Van Kranendonk et al., 2008). The red circle indicates the stratigraphic position of examined stromatolites.
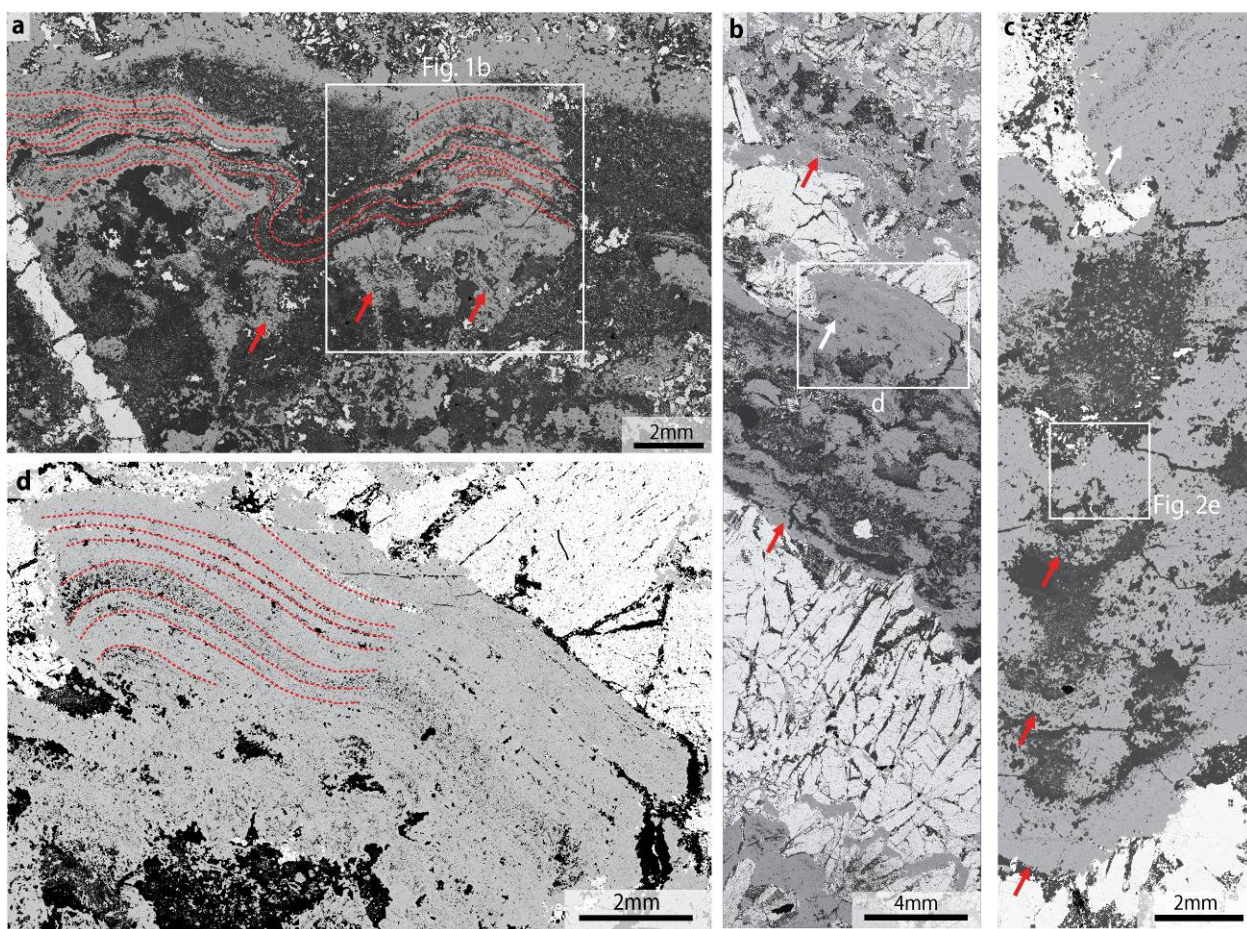
Figure DR2. Scanning Electron Microscopy images of sulfidized Dresser Formation stromatolites. a) Backscattered Electron (BSE) image of stromatolites in sample S1. Note how the basal parts of the stromatolites consist of branching, digitate structures (red arrow). They are capped by columnar structures comprising wavy and wrinkly laminae (red lines). Note the sulfide–barren barite vein (lower left) that cuts across the stromatolites. b–c) Stromatolites in alternation with layers of coarsely crystalline barite in sample S2. Note the stromatolite layers within chert–dolomite (red arrows), and the large sulfide column showing internal lamination (white arrow). Mineralogy is gauged from brightness differences and supported by EDS analysis: white = barite; light grey = sulfide (mainly pyrite ± sphalerite); dark grey = quartz and dolomite. d) BSE image of a strongly sulfidized, finely laminated, columnar stromatolite structure in sample S2; see imaging location in (b). Fine–scale internal lamination is indicated by dashed

lines in the left part of the column. Mineralogy can be gauged from brightness differences: white = barite; light grey = sulfide (mainly pyrite ± sphalerite); dark grey = quartz and dolomite.
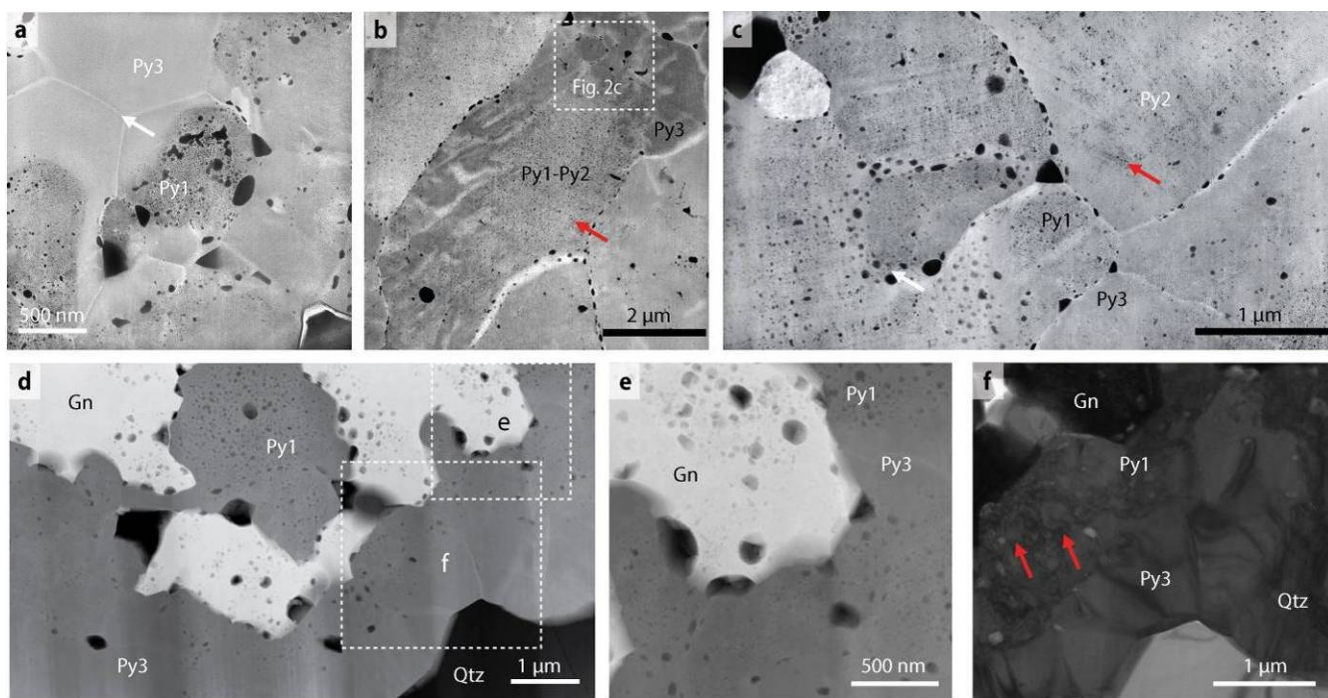
Figure DR3. Scanning Transmission Electron Microscopy (STEM) images of sulfide in the Dresser Formation stromatolites. a) Dark–field STEM image showing irregular nano–porous pyrite (Py1) that is sharply bordered by non–porous, massive pyrite (Py3). The latter shows crystal triple point boundaries (white arrow). b) Image showing the distributions of irregular (Py1) to zoned (Py2) nano–porous pyrite, relative to overgrowths of non–porous, massive pyrite (Py3). Zonation in Py2 is indicated (red arrow). c) Image showing the gradation of pyrite textures: Py1 → Py2 → Py3. Note the void trails along pyrite pseudo–grain boundaries (white arrow), and the zonation in Py2 that is defined by nano–porosity (red arrow). d–e) Image of pyrite intergrown with galena (Gn). Note the nano–porous texture of galena. f) Bright–field STEM image of Py1 that is overgrown by Py3. The red arrows indicate rounded pyrite nano–grains in Py1.
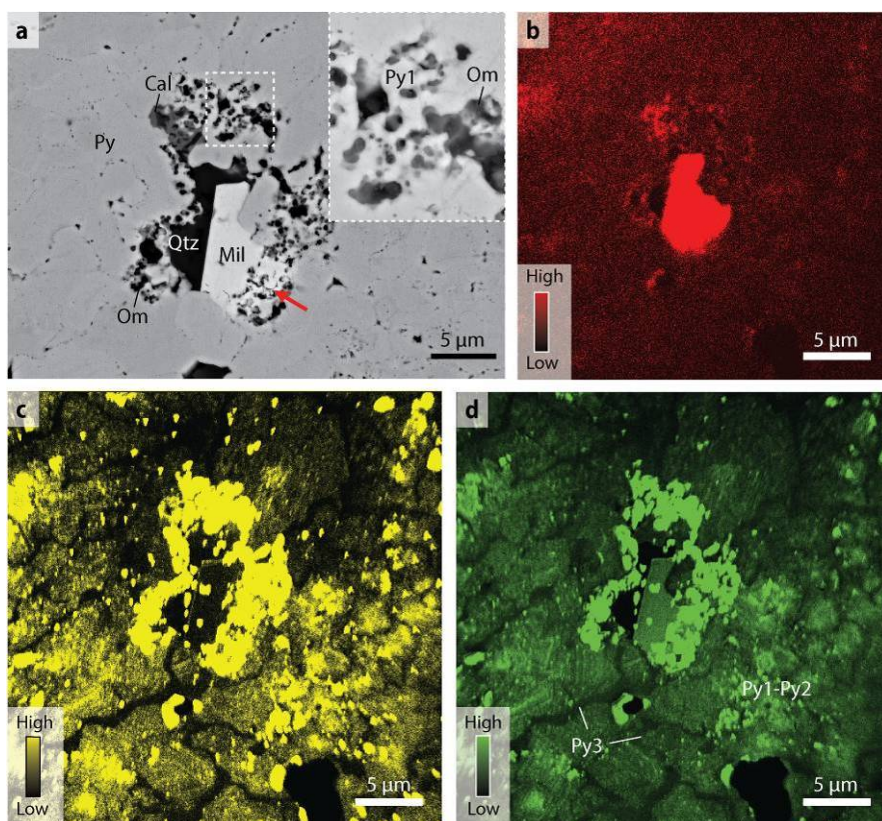
Figure DR4. BSE image and NanoSIMS ion maps of organic matter– (OM–) rich sulfide in the Dresser Formation stromatolites. a) BSE image showing pyrite (Py) plus OM, occurring in association with calcite (Cal), millerite (Mil) and quartz (Qtz). Note the macro–porous pyrite texture that traverses millerite (red arrow). Inset shows OM within pyrite macro–porosity. b–d) Ion maps of Ni (^{58}Ni$^+$), C (^{12}C$^-$) and N (^{26}CN$^-$). Note the enrichment of C and N in assemblages of irregular (Py1) and zoned (Py2) nano–porous pyrite, relative to non–porous, massive pyrite (Py3); compare with Fig. 3a–d.
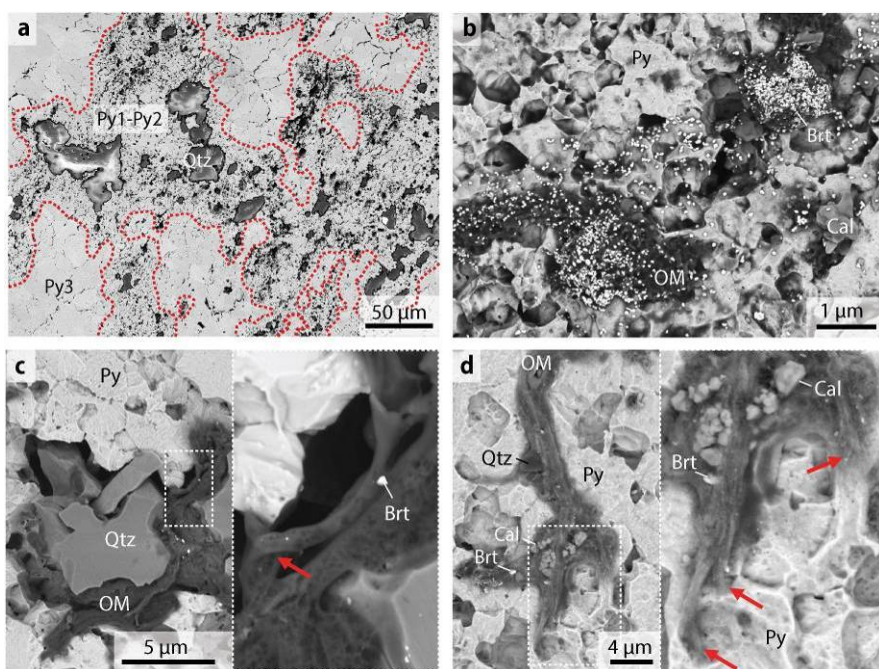
Figure DR5. BSE images of OM in sulfide of the Dresser Formation stromatolites. a) Image of nitric acid etching trails (indicated by red dashed lines) within sulfide, relating to weakly corrosion resistant, irregular (Py1) and zoned (Py2) nano–porous pyrite, plus quartz. These assemblages are overgrown by non–porous, massive pyrite (Py3). b) Irregular structured OM in association with barite and calcite nano–grains. c). Filament bundle around quartz. The inset shows a sinusoidal OM filament twisting around other filaments (red arrow). Note the associated barite nano–grains. d) Branched OM filament bundles speckled by quartz, barite, and calcite nano–grains. Partially pyritized filament branches that pass into pyrite are indicated (red arrows in inset). Brt = barite; Cal = calcite; Py = pyrite; Qtz = Quartz. All images of this figure panel were acquired on nitric acid–etched surfaces.
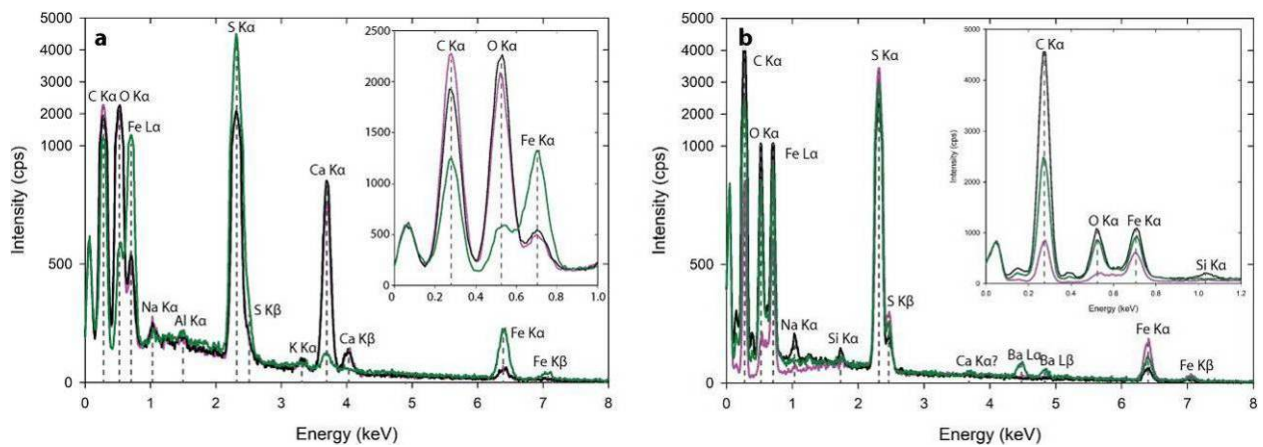
Figure DR6. Chemistry of OM strands and filaments in pyrite of the Dresser Formation stromatolites. a) Energy Dispersive X–ray Spectroscopy (EDS) analyses of the strand in Fig. 4b. The black and pink analyses with high Ca peaks were done on discernible calcite grains in association with OM. The green analysis was done on OM away from calcite grains (asterisk in Fig 4b). Subtle enrichment of Ca and O in the latter analysis indicates partial calcification of OM. b) Analyses of the filament bundle in Fig. 4d. The Ba and Si peaks correspond to the co–analysis of barite and quartz nano–grains. The host of Na is uncertain.

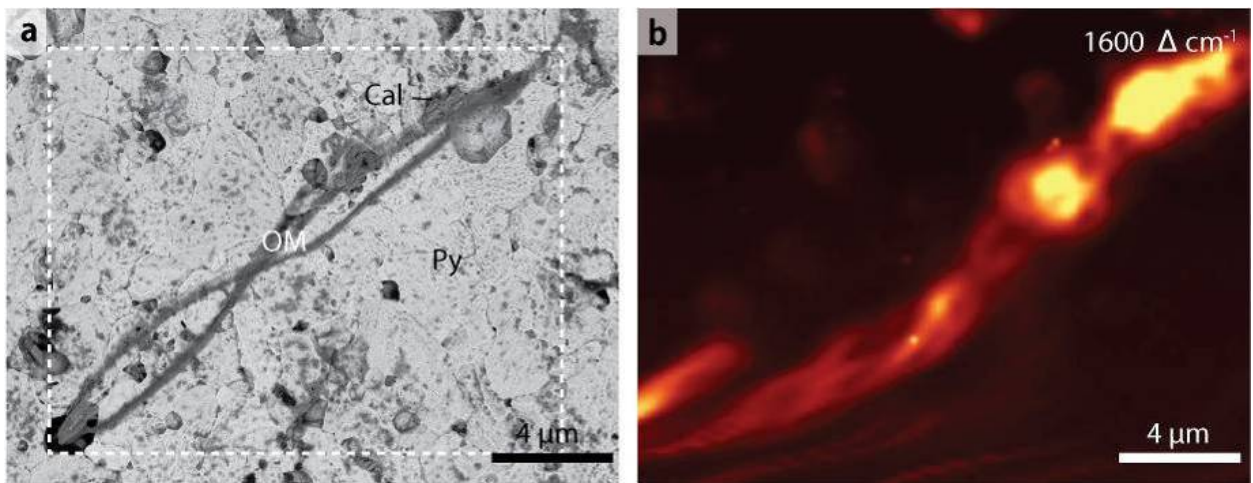Figure DR7. BSE image and a corresponding Raman Spectroscopy map of OM strands in pyrite (compare with Fig. 4b) in pyrite of the Dresser Formation stromatolites. The Raman Spectroscopy map shows the intensity of the G band of OM ($1600\ \Delta\mathrm{cm}^{-1}$ and $50\ \mathrm{cm}^{-1}$ filter width). Note that this map is slightly distorted horizontally at its lower end. Cal = calcite; Py = pyrite.

Methods

Organic Carbon Isotope Analysis

For organic carbon isotope analysis, sample material was crushed into a fine powder using an automated agate mill grinder, which was cleaned with pure quartz sand, ethanol, and distilled water between each run. Approximately 0.1 g of sample powder was dissolved overnight in 5 ml Nitric acid + 5ml HF in a fume hood. Residues were rinsed with Milli–Q water, and then centrifuged several times until they approached a neutral pH condition. A total of 20 mg of decarbonated sample material was loaded into a tin capsule and analyzed using a Thermo Scientific Delta V Plus mass spectrometer coupled to a Flash 2000 elemental analyzer (installed at the Pôle Spectométrie Océan, Brest, France). The isotopic results are reported in delta notation against the V–PDB standard (Vienna Pee Dee Belemnite) with an analytical error of 0.3 ‰.

Scanning Electron Microscopy (SEM) and Energy Dispersive X–ray Spectroscopy (EDS)

Backscattered Electron imagery and EDS analysis was carried out on polished thin sections and epoxy mounts using a FEI XHR–Verios 460L field–emission SEM installed at the Centre for Microscopy, Characterisation and Analysis (CMCA), The University of Western Australia (UWA). Analysis was performed without the use of conductive surface coatings in order to eliminate any possibility of contamination. Imagery was performed using 3 – 20 kV acceleration voltage and 0.1 – 0.8 nA beam current. Up to 15 kV and 0.8 – 1.6 nA was used for EDS analysis. The elements were determined using characteristic Kα and Kβ X–ray emission lines. The EDS data were processed using AZtecEnergy (Oxford Instruments PLC).

Raman Spectroscopy analysis

Raman Spectroscopy analysis of OM was carried out at CMCA, UWA, using a WITec alpha 300RA+ Raman probe combined with a peltier–cooled (– 60 °C) 1024 × 1280 pixel CCD detector, and a Toptica Photonics Xtra II 785 nm laser source. The laser was focused using a 100x/0.9 objective. The laser power was held at << 5 mW in order to minimise risks of thermal

damage of the OM. The data were acquired with 600 l/mm spectral grating in the 100 – 1800 Δcm^{-1} range, and calibrated by analysis of a silicon chip with a characteristic 520 Δcm^{-1} band. The acquisition time for spot analysis was 10 – 15 s with 10 – 15 accumulations. Maps were acquired at ~ 0.25 μm resolution with 0.5 s acquisition time. Project Four (WITec GmbH) was used for background correction and to produce maps by integration over the ~ 1600 Δcm^{-1} (50 Δcm^{-1} filter width) band of OM. Spectral deconvolution in the 1000 – 1700 Δcm^{-1} range was done using Peakfit v.4.12 (Systat Software Inc.), by application of Gaussian–Lorentzian peak fit functions in combination with least–squares methods.

Focussed ion beam (FIB) preparation and Scanning Transmitted Electron Microscopy (TEM)

Site–specific, ultrathin (< 150 nm) TEM wafers of sulfide were prepared using a FEI Helios NanoLab G3 CX DualBeam FIB–SEM installed at CMCA, UWA. Bright–field and dark–field STEM imagery was performed at CMCA, UWA, using a FEI Titan G2 80–200 TEM/STEM with ChemiSTEM Technology. It was operated using 200 kV acceleration voltage.

Nanoscale Secondary Ion Mass Spectroscopy (NanoSIMS) ion mapping

Ion maps were obtained with a CAMECA NanoSIMS 50L at CMCA, UWA. A 5 nm platinum coating provided conductivity. The ion maps were obtained using Cs^+ and O^- sources to detect negative ($^{12}C^-$, $^{16}O^-$ and $^{26}CN^-$) and positive ($^{58}Ni^+$) secondary ions, respectively. For both beam sources, the beam diameter was approximately 100 nm, and the impact energy was 16 keV. The high–resolution O^- beam was obtained with a Hyperion (H200) RF plasma oxygen ion source. The beam current was 3 pA and 50 – 100 pA for the Cs^+ and O^- analyses, respectively. For the Cs^+ analyses, an electron gun was used for charge compensation. The analyses were acquired using raster sizes of ~ 55 μm^2 at 512 × 512 pixel resolution, and 5 – 30 ms dwell time per pixel. Image analysis was done using OpenMIMS.

Nitric–acid Etching

Following textural, mineralogical and chemical examination, the epoxy mounts were ground and repolished, cleaned with ethanol and distilled water, and then locally etched for ~ 60 – 90 s with 70% nitric acid (HNO_3). Etching was done away from epoxy in the centre of the samples in order to eliminate risks of contamination. After rinsing with distilled water and air–drying in an exicator, OM and mineralogy was examined by RS and SEM–EDS without the use of conductive coatings.

References for repository items

Van Kranendonk, M.J., Philippot, P., Lepot, K., Bodorkos, S., and Pirajno, F., 2008, Geological setting of Earth's oldest fossils in the ca. 3.5 Ga Dresser Formation, Pilbara Craton, Western Australia: Precambrian Research, v. 167, p. 93–124.